International Journal of ChemTech Research
CODEN (USA): IJCRGG, ISSN: 0974-4290, ISSN(Online):2455-9555
Vol.9, No.10 pp 90-98, 2016

Photocatalytic hydrogen production from aqueous methanol solution over metallized TiO_2

Luma M. Ahmed[1], Ayad F. Alkaim*[2,3], Ahmed F. Halbus[4],Falah H. Hussein[5]

[1]Department of Chemistry, College of Science, University of Karbala, Karbala, IRAQ
[2]Department of Chemistry, College o f Women Science, University of Babylon, Hilla, IRAQ.
[3]InstitutfürTechnischeChemie, Leibniz Universität Hannover, Callinstrasse 3, D-30167, Hannover, Germany
[4]Department of Chemistry, College of Science, University of Babylon, Hilla, IRAQ
[5]Department of Chemistry, College of Pharmacy, University of Babylon, Hilla, IRAQ

Abstract : In this paper, photocatalytic hydrogen production from aqueous methanol solution with metallized titanium dioxide by platinum and gold is reported. Scherer equation was used to calculate of mean crystallite sizes of bare and metallized TiO_2 via XRD data. The calculated mean crystallite sizes of bare TiO_2 are decreased on metallized it. The AFM images indicate that the shape of bare and metallized TiO_2 is spherical. The particle size was found to be ranging between 9 and 11 crystallite size. The band gap energy for bare TiO_2, Pt(0.5%)/TiO_2 and Au(0.5%)/TiO_2 were calculated after applying the Kubelka-Munk transformation. The results show that there is a shifting from ultra-violet absorption to visible light absorption (red shift) and as a consequence a narrowing in band gap in was observed. The band gap of bare TiO_2 was reduced from 3.289 eV to 3.263eV for Pt(0.5%)/TiO_2 and to 3.246eV for Au(0.5%)/TiO_2. Photoirradiation of argon purged aqueous methanol solution gave hydrogen in the presence of platinum and gold-loaded nanosized titanium dioxide (Hombikat UV 100). The photocatalytic activity of dehydrogenation of aqueous methanol solution of bear and metallized TiO_2 was in the order Pt(0.5%)/TiO_2>Au(0.5%)/TiO_2 while no H_2 evolved when using a bare TiO_2. These results depended significantly on the work function values of Pt (5.93 eV) and for Au (5.31 eV).
Keywords : Hydrogen production; Photocatalytic activity; Pt/TiO_2; Au/TiO_2; Nanoparticle; Methanol.

Introduction

Hydrogen gas comes from either a renewable resource (such as agricultural waste or water), or nonrenewable (fossil fuel or nuclear plant) and hence, it is useful economically and environmentally[1].

Fujishima and Honda[2], first found the hydrogen production from splitting of water molecule using TiO_2, which can generate a photocurrent in an electrochemical cell, employed Pt as the counter-electrode, the essential of photocurrent beyond to produce hole-electron pairs[3-10].

In 1985 Bockris*et al.* reviewed the different possible routes for hydrogen production from water[11]. These routes can be summarized as (Scheme1).

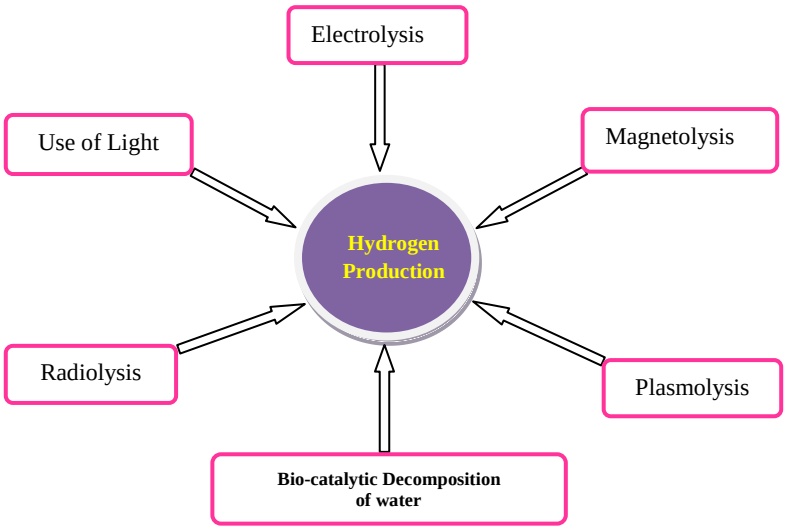

Scheme 1. Some Possible Methods to Produce Hydrogen Gas from Water .

Recently, different methods used for water treatment such adsorption processes[12-19], photocatalysis[20-25], the main advantage in photocatalysis treatment have a good utilization for treatment the wastewater and converted to a clean fuel, such as the process of hydrogen production from water was deemed as an important step in photocatalytic oxidation of methanol, since H_2 is regarded as a renewable resource and natural energy source.Selli *et al.* found that hydrogen can be produced by photocatalytic process of methanol steam reforming over a series of noble metal such as (Ag, Au, Au–Ag alloy and Pt) loaded TiO_2 photocatalyst[26]. However, methanol is oxidized to CO_2 via the formation of formaldehyde and formic acid. Wu and Lee[27] supported the TiO_2 (P 25) by Cu to utilize from photo-oxidation of methanol to produce a hydrogen, and high activity at the optimum loading of nearly 1.2 wt% Cu. Wang *et al.* loaded the surface of metal oxides nanocrystals such as TiO_2, ZnO, CuO, etc. with aluminum for producing hydrogen gas in deionized water and tap water at room temperature, results showed Al loaded TiO_2, Co_3O_4 and Cr_2O_3nanocrystals were very effective to liberate hydrogen gas from deionized water at 25 ^oC[28]. The aim of this work was focused on dehydrogenation of methanol solution to produce hydrogen gas.

2. Experimental

2.1. Materials

All the materials were employed without any further purification. Titanium dioxide type Hombikat UV 100 was supplied by Sachtleben, Germany, that consisted of 100% anatase, with the average diameter of the primary particles was 5-10 nm and BET surface area more than 250 g/ cm^2. Hexachloroplatinic acid hexahydrate (Riedel-De-Haen AG, Seelze, Hannover, Germany),tetrachloroauric acid trihydrate(Riedel-De-Haen AG, Seelze, Hannover, Germany), formaldehyde (40%, Chemanol, Arabia Sudia Kingdom), methanol (HPLC grade, 99.8 %, SdFine-Chem Limited, Mumbai, India), methanol A.R quality (99.85 %, Hayman, England), were used without any further treatment. Deionized water was used in all the experiments.

2.2. Synthesis and characterization of M (Pt; Au)/TiO_2 nanoparticles

In order to get metallized TiO_2, the photodeposition process of 0.5% of platinum or gold on TiO_2 surface was performed by weighting a certain amount of titanium dioxide UV 100 in Pyrex reaction vessel and mixing it in 40 mL of 40% formaldehyde and 10 mL of absolute methanol, followed by the addition of an appropriate amount of as-prepared Pt (1% H_2PtCl_6. 6 H_2O/ 0.1 M HCl) or Au (1% $HAuCl_4$. 3H_2O/ 0.1 M HCl) purged with nitrogen to remove dissolved oxygen, with continuous magnetic stirring (Heidoloph) at 250 rpm.

Then it was irradiated with UV-A light (Philips, 6 lamps Hg lamp, 90 W). The light intensity was 3.49 mW/ cm^2.

The required time for complete photodeposition of gold is double than for complete photodeposition of platinum, i.e., 8 h and 4h respectively.

The milky white suspension turns pale grey with the deposition of Pt and pale purple colour with the deposition of Au. These suspension solution were filtered and washed with absolute methanol. At the end, the product was dried in an oven at 100 ^oC for 2h [24, 25].

The mean crystallite sizes (L) of the bare, Pt(0.5) and Au(0.5) loaded on TiO_2 surface powders were calculated from data of powder X-ray diffraction (Lab X XRD 6000) using Scherrer's formula[29] [26, 27] (Eq. 1) : $L = \frac{k\lambda}{\beta cos\theta}$ (1)

where: L is mean crystallite size, k is a Scherrer's constant (0.94) which depended on the shape of crystal, λ is wavelength of the x-ray radiation (0.15406 nm for Cu kα), β is the full width of half-maximum (FWHM) intensity expressed in radians (originally, β is in degrees multiply by (π/180) to convert it in radians), and θ is a diffraction (Bragg) angle.

The particle sizes of the bare, Pt(0.5) and Au(0.5) loaded on TiO_2 surface were measured by Atomic force microscopy (AFM) using SPM model AA 3000, (Advanced Angstrom Inc.- USA).The crystallinity Index was calculated by using the following equation[30].

$$\boldsymbol{Crystallinity\ Index = \frac{D_p}{L}} \qquad (\mathbf{2})$$

where: D_p is the particle size, which is measured by AFM analysis and Lis mean crystallite size that is calculated by Scherrer equation.

Band gap energies of bare, Pt(0.5%) and Au(0.5%) loaded on TiO_2 surface were determined with reflectance data R by (Cary 100 Scan) using UV-visible spectrophotometer. It was equipped with a Labsphere integrating sphere diffuse reflectance accessory for diffuse reflectance spectra over a range of 300-700 nm employing $BaSO_4$ as a reference material. The measured reflectance data (R) was transformed to the Kubelka-Munk function F(R) from the following equation[31,32]:

$$F(R) = \frac{(1-R)^2}{2R} \qquad (3)$$

$$F(R).E^{1/2} = \left[\frac{(1-R)^2}{2R}.E\right]^{1/2} \qquad (4)$$

The band gap energy for all samples was measured from the plot of $(F(R).E)^{1/2}$ versus (E) (energy of light in eV). It depends on the intersection of tangent via the point of inflection in the absorption band and the photon energy axis.

2.3 Photocatalytic experiments for hydrogen production

The photocatalytic dehydrogenation of aqueous solution of methanol was performed in a double jacket Duran glass reactor. 50 % Methanol with 175 mg/100 mL of M(Au;Pt)/ TiO_2 was irradiation by xenon lamp (Osram XBO-1000 watt) (UV-B light at light intensity 22.00 $mW.cm^{-2}$) under Ar environment for 30 min, at temperature 298.15 K. Before the irradiation, the librated hydrogen gas was determined by using gas chromatography (GC-Shimadzu 8 A, TCD detector) at zero time, and then the solution was irradiated and inert gas (Ar) was passed. The librated hydrogen gas was periodically analyzed by GC instrument using Ar gas as carrier gas and molecular sieve 5 A packed column.

3. Results and discussion

3.1. Characterisation of bare and metallized TiO_2

3.1.1. XRD analysis and AFM analysis

Figure 1 show that no peaks corresponding to platinum and gold were noted by XRD analysis, that indicates to the low loading and high dispersion of metal present in the metallized TiO_2 catalyst[31]. The mean crystallite sizes of the samples were estimated by the Scherrer equation. The calculated values of mean crystallite sizes for bare TiO_2 decreased with metallized from 11.487 nm to 9.355nm and 10.998 for Platinum and gold, respectively. This is due to the location and incorporation of Pt(IV) and Au(III) with Ti(III) in TiO_2 lattice. The ionic radius of Pt(IV) (0.63 Å) is relatively smaller than that of Ti(III) (0.67Å). While Au (III) is incorporated with Ti (III) in TiO_2 lattice, although it has high ionic radius (0.85 Å)[33]. As seen in AFM images in Figure 2, the crystals of bare and metallized TiO_2photocatalyst are spherical particles with ratio of particle sizes about 9–11 crystals. The maximum value of crystallinity index for Pt(0.5)/TiO_2 is 8.233, that referred to suppress a number of crystal defects through decreasing the amorphous phase present in the TiO_2 and rising the photocatalytic activity of TiO_2. The values are presented in Table 1.

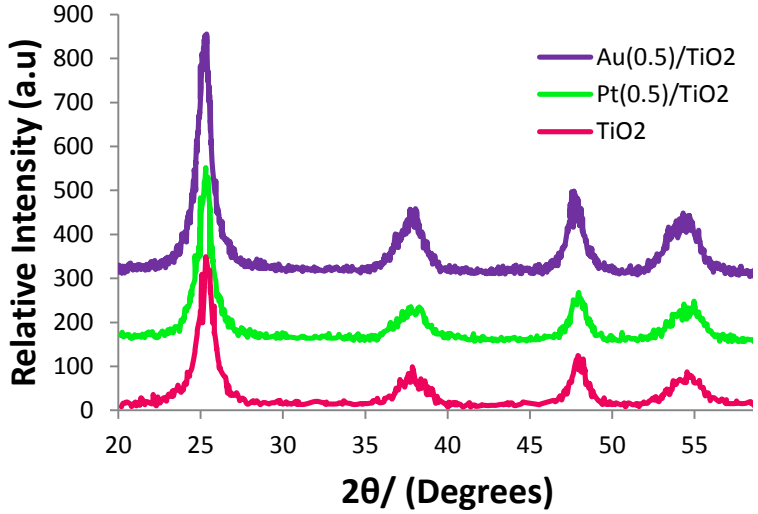

Fig. 1.Powder XRD patterns of (a) bare TiO_2, (b) Pt(0.5)/TiO_2 and (c) Au(0.5)/TiO_2.

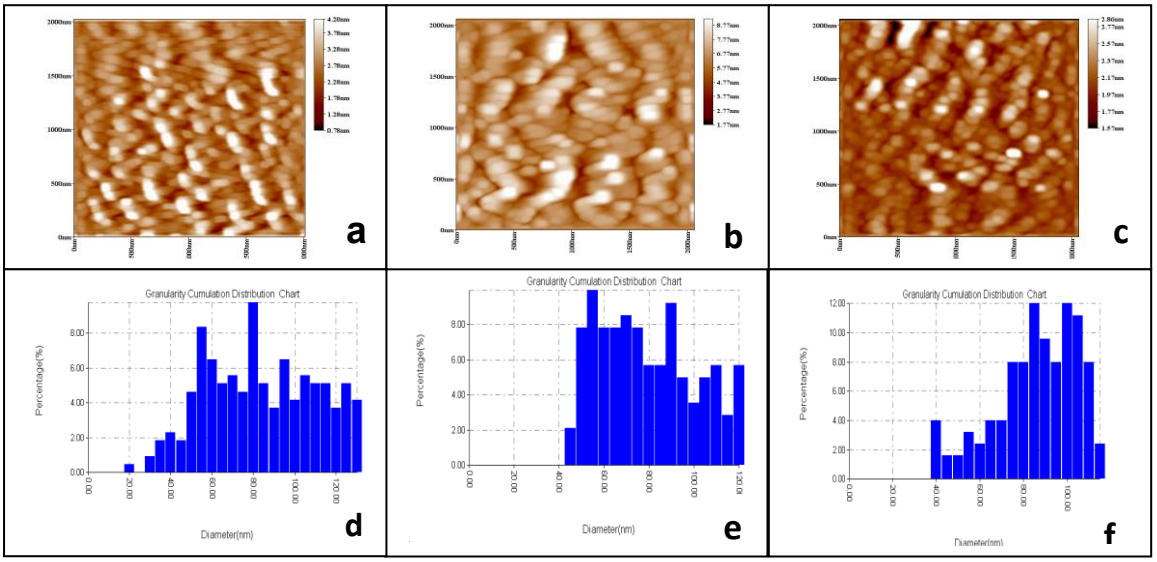

Fig. 2. AFM analysis (a) 2- Dimensions image of bare TiO_2, (b) 2- Dimensions image of Pt(0.5)/ TiO_2, (c) 2- Dimensions image of Au(0.5)/ TiO_2 and (d) Histogram of bare TiO_2, (e) Histogram of Pt(0.5)/TiO_2, (f) Histogram of Au(0.5)/TiO_2 .

Table 1. Characterization of TiO_2, Pt/TiO_2, and Au/TiO_2.

amples	Mean crystallite sizes / nm	Particle sizes / nm	Crystallinity Index
TiO_2	11.487	80.940	7.046
Pt(0.50)/ TiO_2	9.355	77.020	8.233
Au(0.50)/TiO_2	10.998	83.490	7.591

3.1.2. UV-Visible diffuse reflectance

Table 2 indicates that the band gap of bare TiO_2 is larger than that of metallized TiO_2. The effective band gap of $TiO_2$3.289eV is reduced to 3.263 eV and 3.246eV for Pt(0.5)/TiO_2 and Au(0.5)/TiO_2, respectively. This is related to admixing d orbital of Pt and Au with TiO_2 to produce a new intermediate energy levels inside TiO_2 band gap. These results are due to a decrease in Fermi level of TiO_2 and depressing the charge transfer transition from the valence band (mainly formed by 2p orbital of the oxide anions) to the conduction band (mainly formed by 3d t_2g orbital of Ti^{4+}cations). Thereby, the excitation of metallized TiO_2 occurs with lower energy radiation, (red shift)[34], (Figure 3).

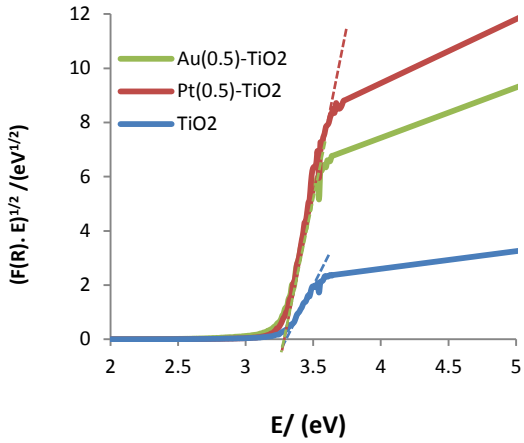

Fig. 3. UV-Visible Kubelka -Munk transformed diffuse reflectance spectra of bare and metallized TiO_2.

Table 2.Band gap measured by UV-Visible diffuse reflectance spectra of bare TiO_2 a metallized TiO_2.

Parameters	TiO_2	$Pt(0.5)/TiO_2$	$Au(0.5)/TiO_2$
λ/ nm	377	380	382
Eg/ eV	3.289	3.263	3.246

3.2. Hydrogen production from methanol solution with metallized TiO_2

Hydrogen production is an important, as it is regarded as a renewable resource and natural energy source. Methanol is a good hydrogen source. The metals have different ability to produce hydrogen gas from photocatalytic dehydrogenation process of methanol.

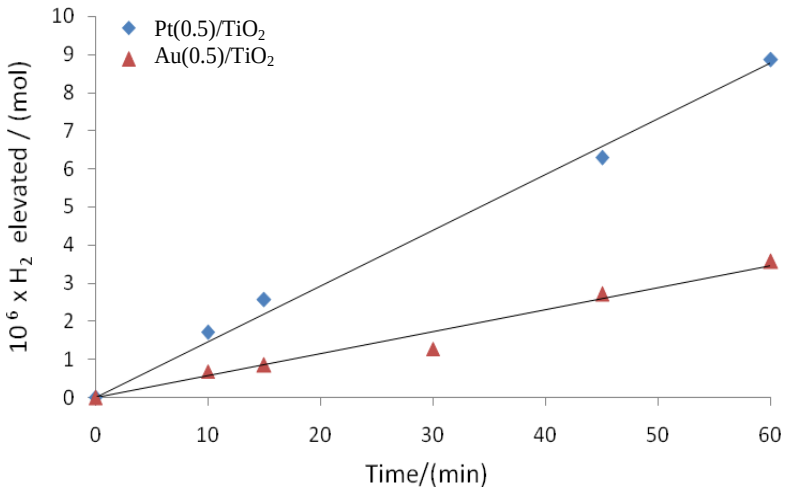

Fig.4. Hydrogen production in photocatalytic dehydrogenation of methanol with Pt(0.5) and Au(0.5) loaded on TiO_2.

Figures 4 shows that the catalyst consisting Pt is more active to produce hydrogen gas than catalyst consisting of Au. That attitude is due to the height of Schottky barrier formed that depends on the values of work functions. The work function of Pt (5.93) is more than that value of the work function of Au (5.31) that will produce a high Schottky barrier height for Pt-TiO_2 contact as compared to Au-TiO_2 contact and therefore, the electrons flowing from TiO_2 to Pt must have energy levels higher than Schottky barrier for Au-TiO_2 contact. The ability for storing the electrons in the Schottky barrier near Pt is the best and increases the separation of photo- generated carriers[34].

3.3. Mechanism of photocatalytic dehydrogenation of methanol solution with metallized TiO_2 in the presence of Argon

When the photon fills on the suspension solution of methanol with metallized TiO_2, the photoelectron is promoted from valance band to conduction band and it created a (e^--h^+) pair. Then the photohole and photoelectron participates in series of reactions according the following equations[35-38].

$$M/TiO_2 + h\nu \longrightarrow (e^- - h^+) \longrightarrow e^- + h^+ \quad (5)$$

$$M_n + e^- \longrightarrow M^-_n \quad (6)$$

$$H_2O \longrightarrow H^+ + {}^-OH \quad (7)$$

$${}^-OH + h^+ {}^{\cdot}OH \longrightarrow H_2O + OH \quad (8)$$

$$CH_3OH + {}^{\cdot}OH \longrightarrow {}^{\cdot}CH_2OH + H_2O \quad (9)$$

${}^{\cdot}CH_2OH$ formed in equation 9 could react either with itself or with hydroxyl radical, which is formed in equation 7.

$$2\,{}^{\cdot}CH_2OH \longrightarrow HCHO + CH_3OH \quad (10)$$

$${}^{\cdot}CH_2OH + {}^{\cdot}OH \longrightarrow HCHO + H_2O \quad (11)$$

H_2O formed in equations 9 and 11 interacts with M^-_n, and the hydroge gas is produced by a process called reverse of hydrogen spillover

$$M^-_n + H_2O \longrightarrow M_n\text{-}H + {}^-OH \longrightarrow M_n + 1/2\,H_2 + {}^-OH \quad (12)$$

The last equation indicates that hydrogen gas is released and ${}^-OH$ is adsorbed on the catalyst surface[39].

4. Conclusion

This study focused on the hydrogen production by photocatalytic dehydrogenation of aqueous methanol solution with metallized TiO_2. The main conclusions can be summarized as follows:

1. The XRD data were used to calculate the mean crystallite sizes of bare and metals percentage (Pt or Au) loaded on TiO_2 surface. The mean crystallite sizes of bare TiO_2 decreased with the increasing metal percentage on TiO_2.
2. AFM images indicate that the shape of bare and metallized TiO_2 are spherical and the particle size is ranged between 9-11 crystals.
3. The band gap decreased with the metal photodeposited on TiO_2.
4. Pt(0.5%)/TiO_2 was more active than Au(0.5%)/ TiO_2 in hydrogen production reaction from aqueous solution of methanol. This is in agreement with their work function values.

References

1. Alkaim A. F., Kandiel T. A., Hussein F. H., Dillert R., and Bahnemann D. W., 2013.Solvent-free hydrothermal synthesis of anatase TiO2 nanoparticles with enhanced photocatalytic hydrogen production activity, Appl. Catal. A-Gen, 466: 32-37.
2. Fujishima A., and Honda K., 1972.Electrochemical photolysis of water at a semiconductor electrode, Nature, 238: 37-38
3. Li, Z.; Wang, Q.; Kong, C.; Wu, Y.; Li, Y.; Lu, G., 2015.Interface Charge Transfer versus Surface Proton Reduction: Which Is More Pronounced on Photoinduced Hydrogen Generation over Sensitized Pt Cocatalyst on RGO?, The Journal of Physical Chemistry C, 119: 13561-13568.
4. Al-Azri, Z. H. N.; Chen, W.; Chan, A.; Jovic, V.; Ina, T.; Idriss, H.; Waterhouse, G. I. N., 2015.The roles of metal co-catalysts and reaction media in photocatalytic hydrogen production: Performance evaluation of M/TiO2 photocatalysts (M = Pd, Pt, Au) in different alcohol–water mixtures, J. Catal., 329: 355-367.
5. Taboada, E.; Angurell, I.; Llorca, J., 2014.Dynamic photocatalytic hydrogen production from ethanol - water mixtures in an optical fiber honeycomb reactor loaded with Au/TiO2, J Catal, 309: 460-467.
6. Serrano D.P., Calleja G., Pizarro P., and Gálvez P., 2014.Enhanced photocatalytic hydrogen production by improving the Pt dispersion over mesostructured TiO2, Int. J. Hydrogen Energy, 39: 4812-4819.
7. Puskelova, J.; Baia, L.; Vulpoi, A.; Baia, M.; Antoniadou, M.; Dracopoulos, V.; Stathatos, E.; Gabor, K.; Pap, Z.; Danciu, V.; Lianos, P., 2014.Photocatalytic hydrogen production using TiO2 - Pt aerogels, Chem. Eng. J., 242: 96-101.
8. Chiarello, G. L.; Dozzi, M. V.; Scavini, M.; Grunwaldt, J.-D.; Selli, E., 2014.One step flame-made fluorinated Pt/TiO2 photocatalysts for hydrogen production, Appl Catal B: Environ, 160-161: 144-151.
9. Wei, P.; Jiawen, J.; Li, Z., 2013.Effect of Pt loading and calcination temperature on the photocatalytic hydrogen production activity of TiO2 microspheres, Ceram. Int., 39: 5387-5391.
10. Montes-Navajas P, Serra M, Garcia H., 2013.Influence of the irradiation wavelength on the photocatalytic activity of Au-Pt nanoalloys supported on TiO2 for hydrogen generation from water, Catal. Sci. Technol., 3: 2252-2258.
11. Bockris, J. O. M.; Dandapani, B.; Cocke, D.; Ghoroghchian, J., 1985.On the splitting of water, International Journal of Hydrogen Energy, 10: 179-201.
12. Aljeboree A. M., Alkaim A. F., and Al-Dujaili A. H., 2015.Adsorption isotherm, kinetic modeling and thermodynamics of crystal violet dye on coconut husk-based activated carbon, Desalin. Water Treat., 53: 3656-3667.
13. Alkaim A. F., Sadik Z., Mahdi D. K., Alshrefi S. M., Al-Sammarraie A. M., Alamgir F. M., Singh P. M., and Aljeboree A. M., 2015.Preparation, structure and adsorption properties of synthesized multiwall carbon nanotubes for highly effective removal of maxilon blue dye, Korean J. Chem. Eng., 32: 2456-2462.
14. Hadi Z. A., Aljeboree A. M. and Alkaim A. F., 2014.Adsorption of a cationic dye from aqueous solutions by using waste glass materials: isotherm and thermodynamic studies, Int. J. Chem. Sci., 12: 1273-1288.

15. Aljeboree A. M., Radi N., Ahmed Z., and Alkaim A. F., 2014.The use of sawdust as by product adsorbent of organic pollutant from wastewater: adsorption of maxilon blue dye, Int. J. Chem. Sci., 12: 1239-1252.
16. Aljeboree A. M., Alshirifi A. N., and Alkaim A. F., 2014.Kinetics and equilibrium study for the adsorption of textile dyes on coconut shell activated carbon, Arabian J. Chem., 10.1016/j.arabjc.2014.01.020.
17. Alkaim A. F., Aljeboree A. M., Alrazaq N. A., Baqir S. J., Hussein F. H., and Lilo A. J. , 2014.Effect of pH on Adsorption and Photocatalytic Degradation Efficiency of Different Catalysts on Removal of Methylene Blue, Asian Journal of Chemistry, 26: 8445-8448.
18. Alkaim A. F., and Alqaragully M. B. , 2013.Adsorption of basic yellow dye from aqueous solutions by Activated carbon derived from waste apricot stones (ASAC): Equilibrium, and thermodynamic aspects, Int. J. Chem. Sc., 11: 797-814.
19. Aljeboree A. M., 2015.Adsorption of methylene blue dye by using modified Fe/Attapulgite clay., Research Journal of Pharmaceutical, Biological and Chemical Sciences 6: 778-788.
20. Enas M. Alrobayi, Abrar M. Algubili, Aseel M. Aljeboree, Ayad F. Alkaim, and Falah H. Hussein, DOI: 10.1080/02726351.2015.1120836.Investigation of Photocatalytic Removal and Photonic Efficiency of Maxilon Blue Dye GRL in the Presence of TiO2 Nanoparticles, Particulate Science and Technology.
21. Karam F. F., Kadhim M. I., and Alkaim A. F. , 2015.Optimal conditions for synthesis of 1, 4-naphthaquinone by photocatalytic oxidation of naphthalene in closed system reactor, Int. J. Chem. Sci., 13: 650-660.
22. Alkaim, A. F., Dillert, R., & Bahnemann, D. W., 2015.Effect of polar and movable (OH or NH2 groups) on the photocatalytic H2 production of alkyl-alkanolamine: a comparative study, Environ. Technol., 36: 2190–2197.
23. Kandiel T. A., Robben L., Alkaim A., and Bahnemann D., 2013.Brookite versus anatase TiO2 photocatalysts: phase transformations and photocatalytic activities, Photochem. Photobiol. Sci., 12: 602-609.
24. Alkaim, A. F.; Kandiel, T. A.; Hussein, F. H.; Dillert, R.; Bahnemann, D. W., 2013.Enhancing the photocatalytic activity of TiO2 by pH control: a case study for the degradation of EDTA, Catal. Sci. Technol., 3: 3216–3222.
25. Alkaim A. F., and Hussein F. H., 2012.Photocatalytic degradation of EDTA by using TiO2 suspension, Int. J. Chem. Sci., 10: 586-598.
26. Chiarello G. L., Aguirre M. H., Selli E., 2011.Hydrogen production by photocatalytic steam reforming of methanol on noble metal-modified TiO2, Journal of Catalysis 273 182–190.
27. Wu, N.-L.; Lee, M.-S., 2004.Enhanced TiO2 photocatalysis by Cu in hydrogen production from aqueous methanol solution, International Journal of Hydrogen Energy, 29: 1601-1605.
28. Wang H., Chung H., Teng H., and Cao G., 2011.Generation of hydrogen from aluminum and water - Effect of metal oxide nanocrystals and water quality, International Journal of Hydrogen Energy, 36: 15136-15144.
29. Patterson, A., 1939.The Scherrer Formula for X-Ray Particle Size Determination, Physical Review, 56: 978-982.
30. Pan, X.; Medina-Ramirez, I.; Mernaugh, R.; Liu, J., Nanocharacterization and bactericidal performance of silver modified titania photocatalyst, Colloids and Surfaces B: Biointerfaces, 77: 82-89.
31. Patterson, A. L., 1939.The Scherrer Formula for X-Ray Particle Size Determination, Physical Review, 56: 978-982.
32. Boroumand, F.; Moser, J. E.; van den Bergh, H., 1992.Quantitative Diffuse Reflectance and Transmittance Infrared Spectroscopy of Nondiluted Powders, Applied Spectroscopy, 46: 1874-1886.
33. Choudhury, B.; Borah, B.; Choudhury, A., Ceâ€“Nd codoping effect on the structural and optical properties of TiO2 nanoparticles, Materials Science and Engineering: B, 178: 239-247.
34. Ahmed L. M., Ivanova I., Hussein F. H., and Bahnemann D. W. , 2014.Role of Platinum Deposited on TiO2 in Photocatalytic Methanol Oxidation and Dehydrogenation Reactions, International Journal of Photoenergy, Volume 2014 (2014): Article ID 503516, 503519 pages.
35. Wang C., Pagel R., Bahnemann D. W., and Dohrmann J. K., 2004.Quantum Yield of Formaldehyde Formation in the Presence of Colloidal TiO2-Based Photocatalysts: Effect of Intermittent Illumination, Platinization, and Deoxygenation, J. Phys. Chem. B, 103: 14082–14092.

36. Kandiel T.A., Dillert R., Robben L., Bahnemann D.W. , 2011.Photonic efficiency and mechanism of photocatalytic molecular hydrogen production over platinized titanium dioxide from aqueous methanol solutions, Catal. Today, 161: 196-201.
37. Ismail A. A., D.W. Bahnemann D. W., 2009.Synthesis of TiO2/Au nanocomposites via sol-gel process for photooxidation of methanol, Journal of Advanced Oxidation Technologies, 12: 9-15.
38. Wang C., Rabani J., Bahnemann D. W., and Dohrmann J. K., 2002.Photonic efficiency and quantum yield of formaldehyde formation from methanol in the presence of various TiO2 photocatalysts, Journal of Photochemistry and Photobiology A: Chemistry, 148: 169-176.
39. Raheem RA, Al-gubury HY, Aljeboree AM, Alkaim AF. Photocatalytic degradation of reactive green dye by using Zinc oxide. journal of Chemical and Pharmaceutical Science. 2016; 9: 1134-1138.

*****